

OPEN

16S rRNA gene sequencing reveals an altered composition of the gut microbiota in chickens infected with a nephropathogenic infectious bronchitis virus

Puzhi Xu^{1,3}, Yan Shi^{2,3}, Ping Liu¹, Yitian Yang¹, Changming Zhou¹, Guyue Li¹, Junrong Luo¹, Caiying Zhang¹, Huabin Cao¹, Guoliang Hu¹ & Xiaoquan Guo^{1*}

Infectious bronchitis virus (IBV), a member of the Coronaviridae family, causes serious losses to the poultry industry. Intestinal microbiota play an important role in chicken health and contribute to the defence against colonization by invading pathogens. The aim of this study was to investigate the link between the intestinal microbiome and nephropathogenic IBV (NIBV) infection. Initially, chickens were randomly distributed into 2 groups: the normal group (INC) and the infected group (IIBV). The ilea were collected for morphological assessment, and the ileal contents were collected for 16S rRNA gene sequencing analysis. The results of the IIBV group analyses showed a significant decrease in the ratio of villus height to crypt depth ($P < 0.05$), while the goblet cells increased compared to those in the INC group. Furthermore, the microbial diversity in the ilea decreased and overrepresentation of *Enterobacteriaceae* and underrepresentation of *Chloroplast* and *Clostridia* was found in the NIBV-infected chickens. In conclusion, these results showed that the significant separation of the two groups and the characterization of the gut microbiome profiles of the chickens with NIBV infection may provide valuable information and promising biomarkers for the diagnosis of this disease.

Based on the revolution in our understanding of host-microbial interactions in the past two decades, it has been recognized that the gut microbiome is exceedingly complex¹. We have at least 100 trillion (10^{14}) microbial bacteria and a quadrillion viruses in and on us². Collectively, the microbial bacteria that are located in and on the body make up our microbiota, and the genes they encode are recognized as our microbiome. Numerous studies have shown that the role of intestinal flora includes nutrient absorption, mucosal barrier fortification, xenobiotic metabolism, angiogenesis, immunity, and response to infection³⁻⁵. In human studies, many diseases are closely related to anomalies of the intestinal microbial community, comprising of liver cirrhosis, allergies, obesity, diabetes and so on⁶⁻⁸. Indeed, indigenous microbiota play a crucial part in the prevention and therapy of microbial infections and are frequently referred to as a “forgotten organ”^{1,9,10}. Our recognition of the gut microbiota and the identification of its composition when contrasted between diseased and healthy states allow the determination of dysbacteriosis, which may be associated with disease progression; thus, this may serve as a new way to diagnose, prevent and treat interventions¹¹.

Although the ileum microbiota is comparatively stable under normal conditions, it is readily affected by various diseases^{12,13}. The gut dysbacteriosis induced by viruses might promote the replication and transmission of viruses in organisms; this phenomenon has been found for simian immunodeficiency virus (SIV) and human immunodeficiency virus (HIV)^{14,15}. Infectious bronchitis virus (IBV), which can cause a highly infectious respiratory disease and urogenital illness characterized by gout or nephritis in chickens, is a gamma coronavirus in the family Coronaviridae^{16,17}. All IBV strains can infect a wide range of chicken epithelial surfaces, such as the trachea, kidney,

¹Jiangxi Provincial Key Laboratory for Animal Health, College of Animal Science and Technology, Jiangxi Agricultural University, Nanchang, Jiangxi, China. ²School of Computer and Information Engineering, Jiangxi Agricultural University, Nanchang, Jiangxi, China. ³These authors contributed equally: Puzhi Xu and Yan Shi. *email: xqguo20720@aliyun.com

proventriculus and intestines¹⁸. Some IBV strains are called nephropathogenic IBV (NIBV) because they lead to severe kidney infections in addition to respiratory infections. It is noteworthy that IBV was detectable in intestinal epithelial cells¹⁹. Many studies point out that the chicken ileum is a significant location for digestion and nutrient absorption and is home to a diverse microbial community^{20,21}. However, there has been little exploration of the alteration in the gut microbial community structure and abundance in chickens with IBV infection. Thus, there is an urgent need to establish the aetiological link between the IBV and gut microbiota. Here we investigated the ileum microbiome in chickens infected with IBV for a more detailed and comprehensive evaluation.

The exploration of the chicken intestinal microbiota has primarily been researched by culture-based methods²². However, these methods have limitations: they are inapplicable to nonculturable bacteria and are selective for readily cultivated bacteria¹³. To address these limitations, molecular techniques have been used to characterize the intestinal microbiota. Illumina sequencing of single or multiple hypervariable region amplification in the 16S rRNA gene is an effective approach for gut microbiome analysis²³. In the present study, we elucidated the effects of NIBV infection on the chicken gut microbiome by 16S rRNA gene sequencing. The relative abundance data from the ileum microbiome suggested differences between chickens in the INC group and those in the IIBV group infected with NIBV. Therefore, further investigation into the mechanism of this shift will help us understand IBV infection and provide a potential approach to diagnose, treat and prevent interventions.

Results

Viral load and histopathology. All the NIBV-infected chickens in the IIBV group were listless, huddled together, had watery faeces, and displayed ruffled feathers (score = 2, according to the methods described by Avellaneda *et al.*²⁴) from 3 to 9 days post-inoculation (dpi), and the morbidity was higher than 90%. These clinical symptoms were not observed in the INC group. The quantification of the viral load by RT-qPCR showed values ranging from 2.96×10^3 to 3.84×10^8 genomic copies per $0.2 \mu\text{g}$ of RNA, with the lowest viral load in the jejunum and the highest in the kidneys (Fig. 1B). It was noted that the viral load in the ileum was much higher than that in the jejunum, reaching 1.39×10^5 genomic copies per $0.2 \mu\text{g}$ of RNA. No viral RNA was detected in the INC group. There were more goblet cells, which appeared as vacuoles when stained by H&E, in the IIBV group than in the INC group (Fig. 1C, red arrow). In addition, there were many shed villus epithelial tissue that appeared in the ileum of the IIBV group (Fig. 1C, black arrow). Among the ileum, there was no significant difference in villus height (Student's t test, $P = 0.094$, Fig. 1D), but crypt depth was significantly increased (Student's t test, $P = 0.0003$, Fig. 1E), and the V/C ratio was significantly decreased (Student's t test, $P = 0.016$, Fig. 1F).

Description of the sequencing data. After two separate runs on an Illumina HiSeq. 2500 platform and quality-filtering as described in the methods, 698,855 total sequences were identified for further analysis. The rarefaction curves (Fig. 2a) showed that the sequencing depth was near saturation and that the sequencing data included most of the 16S rRNA gene information in the samples.

A decrease in the microbial diversity in the ileum of chickens with NIBV infection. The sample community richness was evaluated based on the operational taxonomic units (OTU)²⁵ counts in each single sample as shown in Table 1. As shown by the OTU counts, the number of OTUs in the ileum of the IIBV group chickens was less than that of the INC group chickens (Fig. 2b). According to the lower ACE and Chao1 indices, NIBV infection reduced the community richness compared to that in the INC group (Table 1). In addition, neither the Shannon nor the Simpson indices were significantly different between the IIBV group and the INC group within the experiment (Wilcoxon, $P = 0.5887$ and $P = 0.9372$, respectively). The higher Shannon and Simpson index indicated a higher bacterial diversity, which meant that the NIBV infection decreased the microbial diversity compared to that in the INC group (Fig. 2c,d). In conclusion, these data indicated a smaller bacterial diversity in the ileal microbiota of NIBV infected chickens.

NIBV infection altered the ileal bacterial microbiome composition in chickens. To compare the global differences in the bacterial community composition between the NIBV infected chickens and the INC group chickens, the Bray-Curtis similarity and unweighted UniFrac²⁶ were calculated (Fig. 3a). We also performed nonmetric multidimensional scaling (NMDS)²⁷ of all the samples using count-based Bray-Curtis similarity at the OTU level to explore the differences in the bacterial community composition among the two main groups of chickens²⁸. As shown in Fig. 3b, the results provided good discrimination between the groups, suggesting that the bacterial community composition of the IIBV group was different from that of the INC group. Simper (similarity percentage) is a decomposition of the Bray-Curtis difference index, which quantifies the contribution of each species to the difference between the two groups. The results showed the top 10 species in the genus level and their contributions to the differences between the two groups (Fig. 3c).

We utilized principal coordinate analysis (PCoA) to visualize visualizing the similarity of the microbial community structures and the phylogenetic distances between the samples by using the phylogenetic-tree-based weighted UniFrac metric. Figure 3d is a UniFrac PCoA-based comparison of the microbial community from the ileum, showing that the NIBV-infected chickens and the normal chickens had a clear separation. In addition, analysis of similarity (ANOSIM) based on the Bray-Curtis distance (R-value = 0.413, $P = 0.002$, Fig. 3e) and analysis of molecular variance²⁹ based on the weighted UniFrac distance (P -value = 0.027, AMOVA) showed a significant separation of the two groups. These results suggested distinct differences in the bacterial composition between the INC group and IIBV group.

An inspection of the predicted taxonomic profiles at the phylum level for all the samples indicated that *Firmicutes* (82.3%) was the major phylum of the ileal community, exceeding *Proteobacteria* (9.6%) and *Bacteroidetes* (4.3%). Notably, at the phylum level, the abundance of *Firmicutes* decreased (from 89.21% to 75.44%) in the IIBV group compared to that in the INC group, whereas there was an increase in the abundances of *Proteobacteria* (from 2.36%

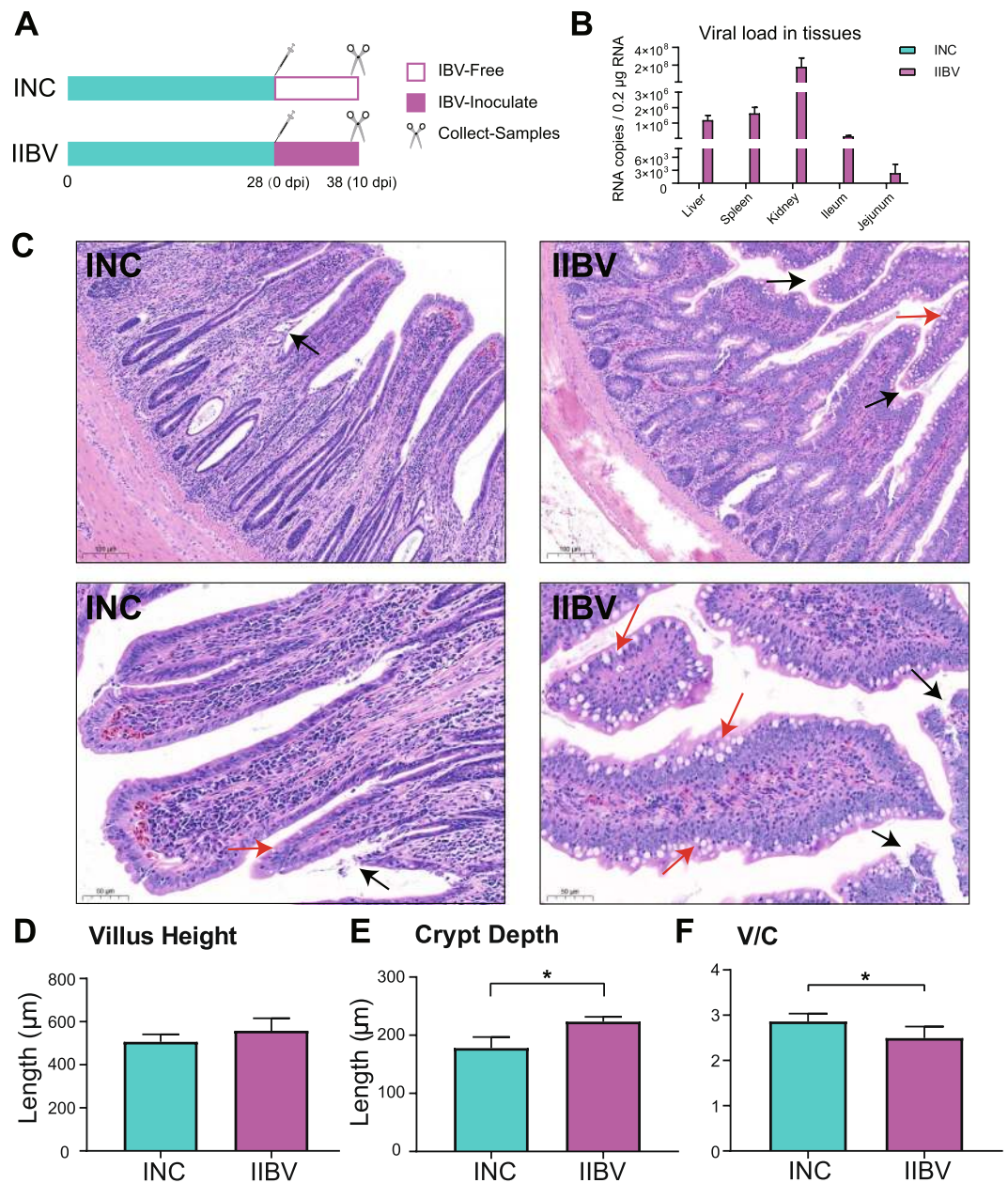


Figure 1. Changes in chickens with SX9 infection. (A) Experimental design, including viral inoculation time and sample collection time. (B) Viral load in different chicken tissues quantified by RT-qPCR (n = 6). (C) Histopathological changes in the ilea of chickens challenged with the NIBV strain SX9 [H&E staining]. The black arrow shows the shed villus epithelial tissue, and the red arrow shows the goblet cells (vacuole). The villus height (D) and crypt depth (E) and the ratio of the villus height to the crypt depth (V/C) (F) of the ilea were measured by Image-Pro Plus 6.0. The data are shown as the means, with SEMs in (D to F). The asterisk superscripts on the bars indicate significant differences compared with the control group (t test, *P < 0.05).

to 16.89%) and *Bacteroidetes* (from 1.91% to 6.69%) (Fig. 4a). Evidently, *Lactobacillaceae*, belonging to the phylum *Firmicutes*, was the most abundant family in the ileum. The family *Clostridiaceae 1* had significantly lower abundance in the IIBV group than in the INC group (P < 0.05) (Fig. 4b). *Lactobacillus*, belonging to the family *Lactobacillaceae*, was the most abundant genus in the ilea. The genus *Candidatus Arthromitus*, belonging to the phylum *Firmicutes*, and the genus *unidentified Chloroplast*, belonging to the phylum *Cyanobacteria*, were significantly less abundant in the IIBV group than in the INC group (P < 0.05) (Fig. 4c).

The linear discriminant analysis effect size (LEfSe) analysis was performed in this study to identify distinctive features between the two groups³⁰. The differentially abundant phyla detected showed that the *Cyanobacteria* phylum was predominant in the INC group, while the most abundant phylum in the IIBV group was *Proteobacteria* (Fig. 5a). For the IBV-infected chickens, there was an overrepresentation of *Enterobacteriaceae* and underrepresentation of *Chloroplast* and *Clostridia* (Fig. 5b).

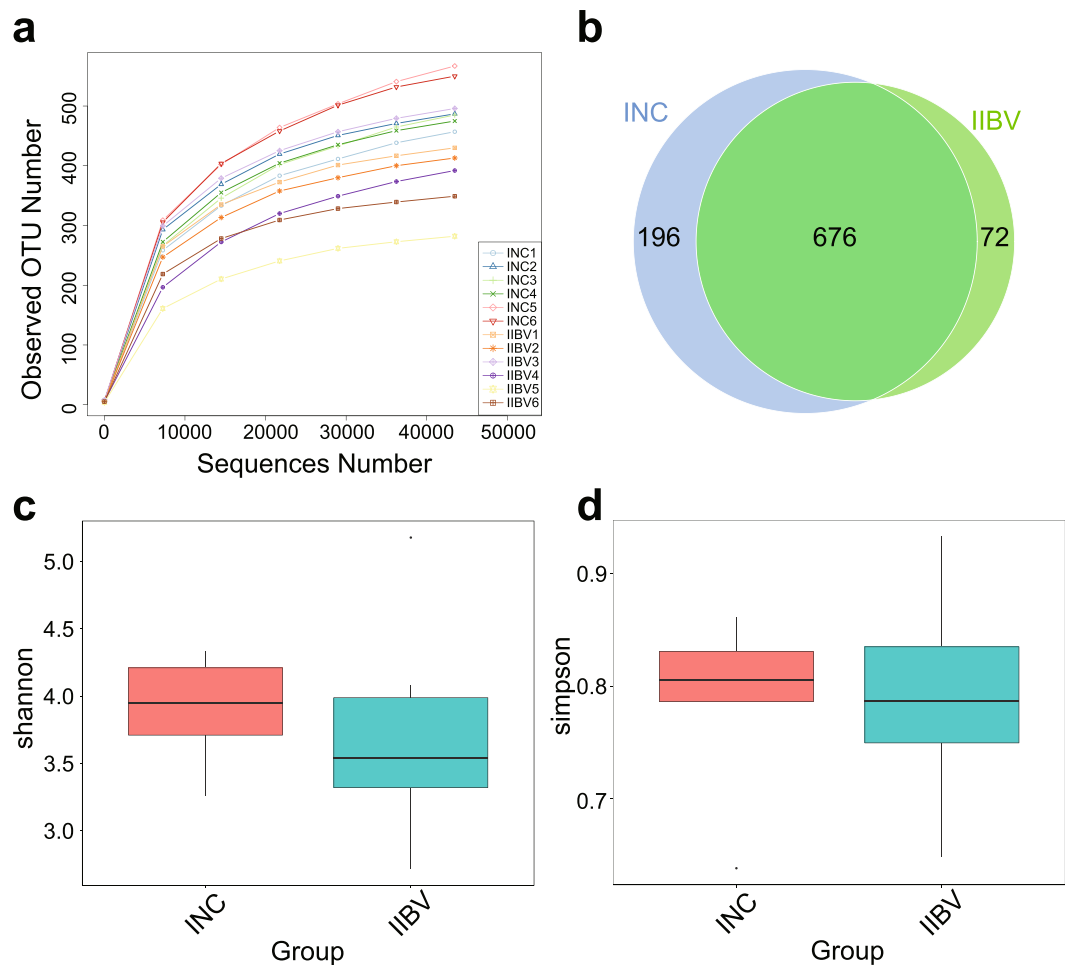


Figure 2. Sample abundance and evaluation of the alpha diversity. **(a)** Rarefaction curves of the OTU number in the INC and IIBV groups ($n = 6$ per group). The number of sequences sampled represents the number of sequencing reads, which were clustered into operational taxonomic units (OTUs) at 97% similarity. **(b)** Venn diagram showing the overlap in the differential abundance of the OTUs in the control and NIBV-infected chickens. The bacterial diversity in the INC and IIBV groups was estimated by the Shannon index **(c)** and Simpson index **(d)**. The results were compared using a Wilcoxon test.

Sample	Reads	OTUs	Shannon	Simpson	Chao1	ACE	Goods Coverage
INC1	69,809	457	3.258	0.638	541.726	536.081	0.998
INC2	67,468	487	4.014	0.786	523.181	537.556	0.998
INC3	63,114	485	3.654	0.824	567.179	585.597	0.997
INC4	59,820	475	3.879	0.787	533.897	536.607	0.998
INC5	69,855	567	4.332	0.833	757.815	718.399	0.996
INC6	61,207	550	4.276	0.861	602.009	620.741	0.998
IIBV1	45,655	430	3.706	0.802	466.849	464.887	0.999
IIBV2	52,163	413	4.083	0.846	452.276	455.064	0.998
IIBV3	55,708	496	5.178	0.933	549.915	557.015	0.998
IIBV4	49,563	392	3.301	0.772	458.944	465.737	0.998
IIBV5	51,018	282	2.717	0.648	296.138	305.69	0.999
IIBV6	53,475	349	3.38	0.742	371.021	373.35	0.999

Table 1. Number of OTUs per groups and estimate of sequence diversity and richness.

Predicted metagenomic functions showed the effects of the NIBV infection. To gain insight into the relationship between NIBV infection and gut microbiome functions, Phylogenetic Investigation of Communities by Reconstruction of Unobserved States (PICRUSt)³¹ was implemented to predict the potential

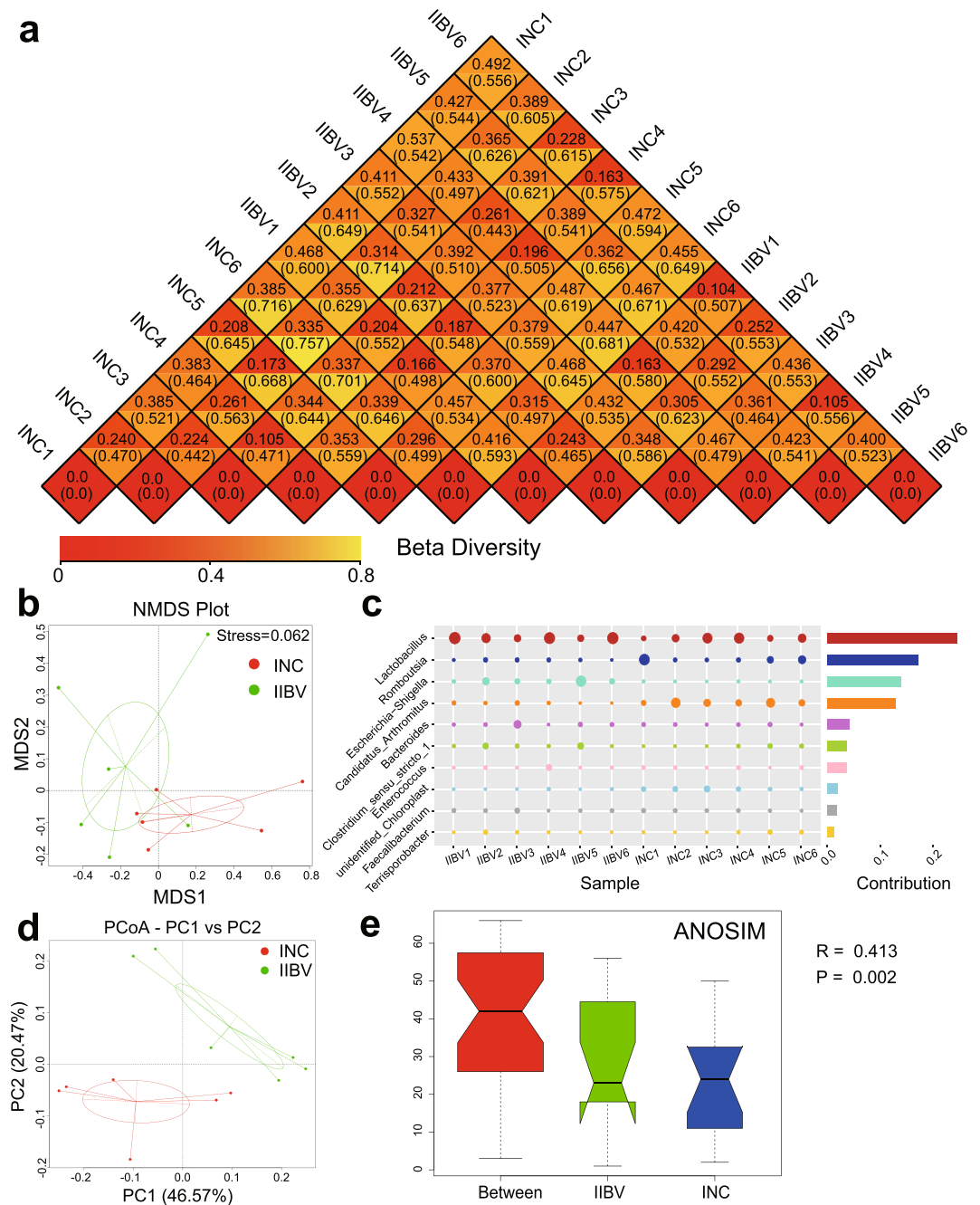


Figure 3. Exploration of the beta diversity in the INC and IIBV groups. **(a)** Beta diversity index heatmap. The number in each square is the difference coefficient between the two samples. The smaller the difference coefficient is, the smaller the difference in species diversity. In the same square, the upper and lower values represent the weighted and unweighted UniFrac distances. **(b)** The nonmetric multidimensional scaling (NMDS) plot, showing the difference in the bacterial communities according to the Bray-Curtis distance. **(c)** Ten species (at the phylum level) with the highest contributions to the difference in the bacterial communities based on Simper analysis and Bray-Curtis distance. **(d)** Principal coordinate analysis (PCoA) plot of the similarities between the different groups derived based on UniFrac distance. Principal components (PCs) 1 and 2 explained 46.57% and 20.47% of the variance, respectively. **(e)** Analysis of similarities (ANOSIM) of the bacterial communities of the ileal samples between the INC and IIBV groups based on Bray-Curtis distance ($R = 0.43 > 0$ indicates that the differences between the groups are significant, $P = 0.002$ indicates that the statistics are significant).

metagenomes from the community profiles of the normalized 16S rRNA genes (Fig. 6). The results showed that there were sixteen pathways from level 3 of the Kyoto Encyclopaedia of Genes and Genomes (KEGG, <http://www.genome.jp/kegg/>) enriched in the INC group ($P < 0.01$, White's non-parametric t-test): atrazine degradation;

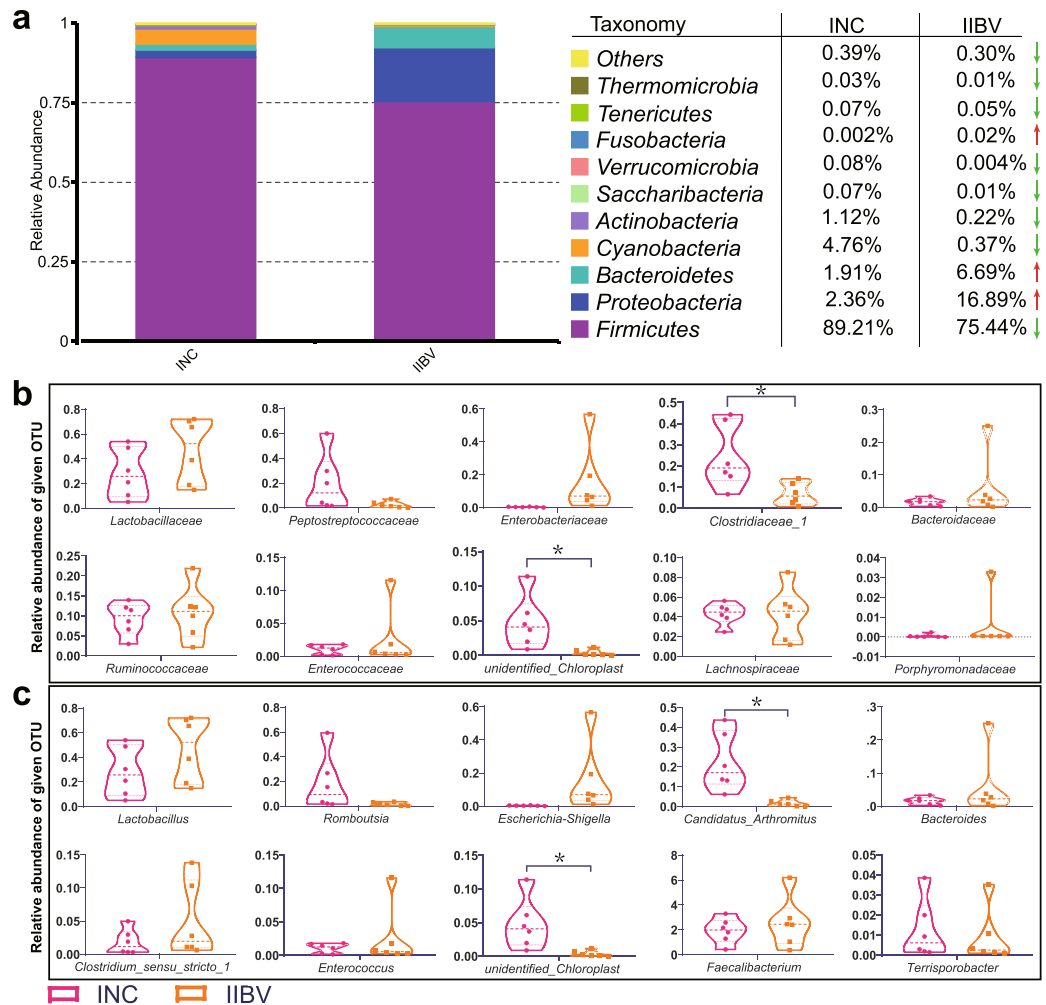


Figure 4. Aggregate microbiota composition at different levels in the INC and IIBV groups. **(a)** Bar plot of the identified bacterial phylum in the analysed samples. The legend reports the average of the relative abundance of each phylum in both animal groups. The abundance of bacteria is shown at the family **(b)** and genus **(c)** levels. Only the families and genera with the top 10 highest abundances were plotted (t test, * $P < 0.05$).

stilbenoid, diarylheptanoid and gingerol biosynthesis; meiosis-yeast; flavonoid biosynthesis; amoebiasis; amino acid metabolism; ether lipid metabolism; plant-pathogen interaction; lipid biosynthesis proteins; tuberculosis; steroid biosynthesis; sporulation; fatty acid biosynthesis; ABC transporters; chlorocyclohexane and chlorobenzene degradation; and N-glycan biosynthesis. Six pathways were enriched in the IIBV group: other ion-coupled transporters; secondary bile acid biosynthesis; primary bile acid biosynthesis; nucleotide metabolism; nicotinate and nicotinamide metabolism; and toluene degradation (Fig. 5). Altogether, these data suggest that IIBV infection alters the metabolic functions of ileal microbiota and therefore deserves further investigation.

Discussion

The gut microbiome contains very diverse bacteria and influences myriad host functions²⁸. Under pathological conditions, the microbial community composition changes, including an increase and decrease in bacterial populations, causing changes in a wide range of metabolic functions^{32,33}. Accordingly, it is certainly necessary to understand the bacterial community composition and changes in gut microbiota with IBV infection. However, the composition of the gut microbiota and how the coronavirus can affect the gut microbiota are still unclear. Therefore, the effects of IBV infection on chicken ileum damage and the ileum microbiome were investigated in our study by using 16S rRNA gene sequencing. 16S rRNA gene sequencing has been applied extensively for assessing the phylogenetic distribution of metagenomes. It is known that the bacterial 16S rRNA gene consists of nine hypervariable regions, and sequences generated by applying different combinations of these regions generally present differing profiles of microbial diversity. Therefore, the optimal choice of the hypervariable region(s) and primer combination vary between various ecological communities. Previous research proved that the highest bacterial diversity and species richness in chicken gut microbiomes were obtained using the primer set corresponding to the V3-V4 region^{34,35}. Based on these investigations, in our study, we selected primers targeting the V3-V4 regions of the 16S rRNA gene.

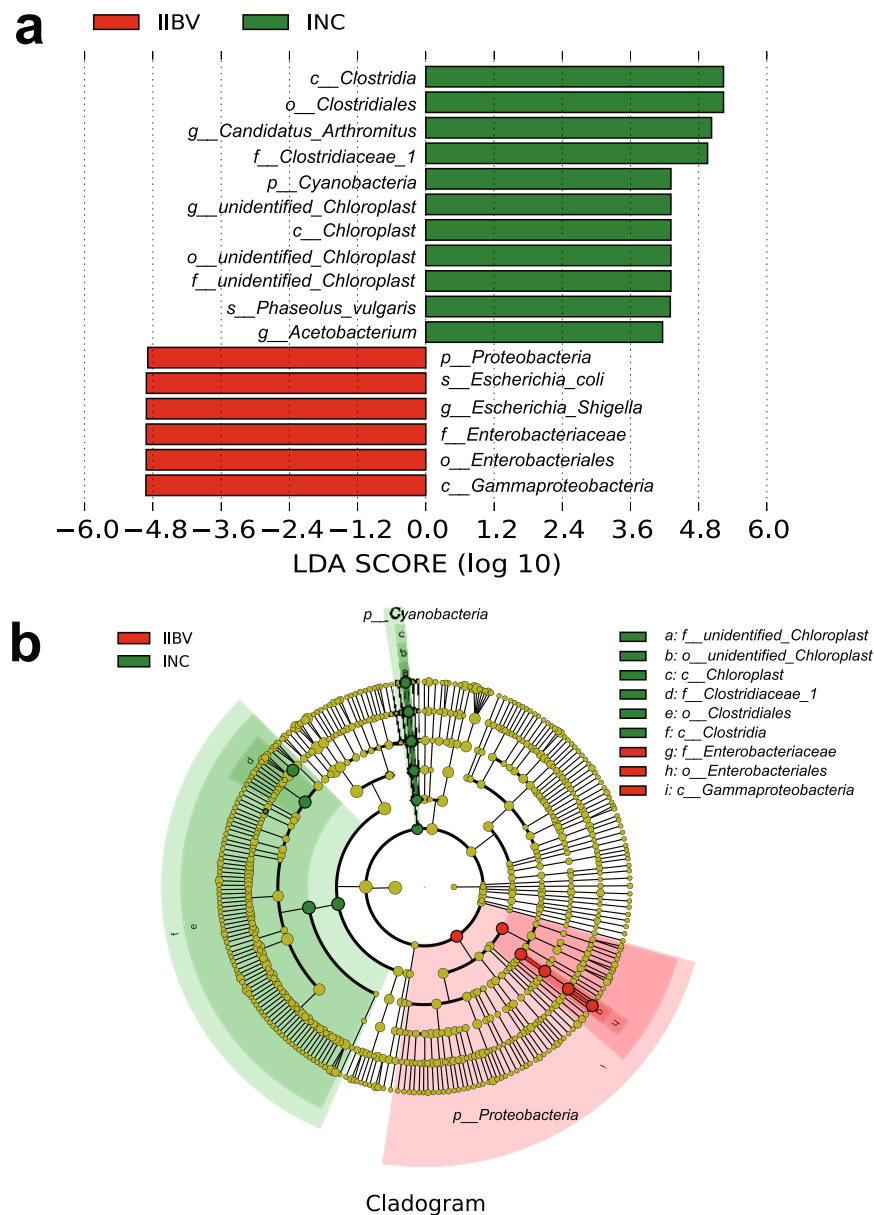


Figure 5. Different structures of gut microbiota in the INC and IIBV groups, according to the LEfSE analysis. **(a)** Taxonomic biomarkers found in the INC (green) and IIBV (red) groups by linear discriminant analysis effect size (LEfSE). **(b)** Cladogram plot of the biomarkers. The size of the node represents the abundance of the taxa. Only taxa with LDA scores (log 10) > 4 are shown.

The complete intestinal structure is essential for digestive and absorptive functions which are intimately associated with the morphological transformations in villus length and crypt depth^{36,37}. In the current study, NIBV infection increased the crypt depth and lowered the ratio of villus height to crypt depth in the ileum compared to those in the INC group. These findings suggest that NIBV infection can destroy intestinal mucosal integrity and may slow the growth of intestinal villus epithelial cells. Furthermore, it was reported that intestinal goblet cells play a crucial defensive role in the intestine by synthesizing and secreting several mediators, including mucins and trefoil factor family peptides, which serve defensive and healing functions in the gut^{38–40}. In this study, NIBV infection obviously increased the number of goblet cells compared to that in the normal group, which indicated hyperplasia of the goblet cells in the ileum during NIBV infection and may be associated with microbial challenges.

Higher diversity and integrity of gut microbiota is favourable to the intestinal ecosystem^{41,42}. According to recent research, viral infection can lower microbial diversity in the gut microbiota according to recent research^{43–45}. Consistent with previous findings, in this study, our results demonstrated that NIBV infection decreases the diversity and richness of gut microbiota (Fig. 2c and Table 1). The analysis of the taxonomic composition displayed a reduction in the *Firmicutes* and *Cyanobacteria* phyla and an enrichment of the phylum *Proteobacteria* and *Bacteroidetes* in the ilea. Importantly, the relative abundance of *Enterobacteriaceae*, particularly *E. coli*, was increased in the ilea

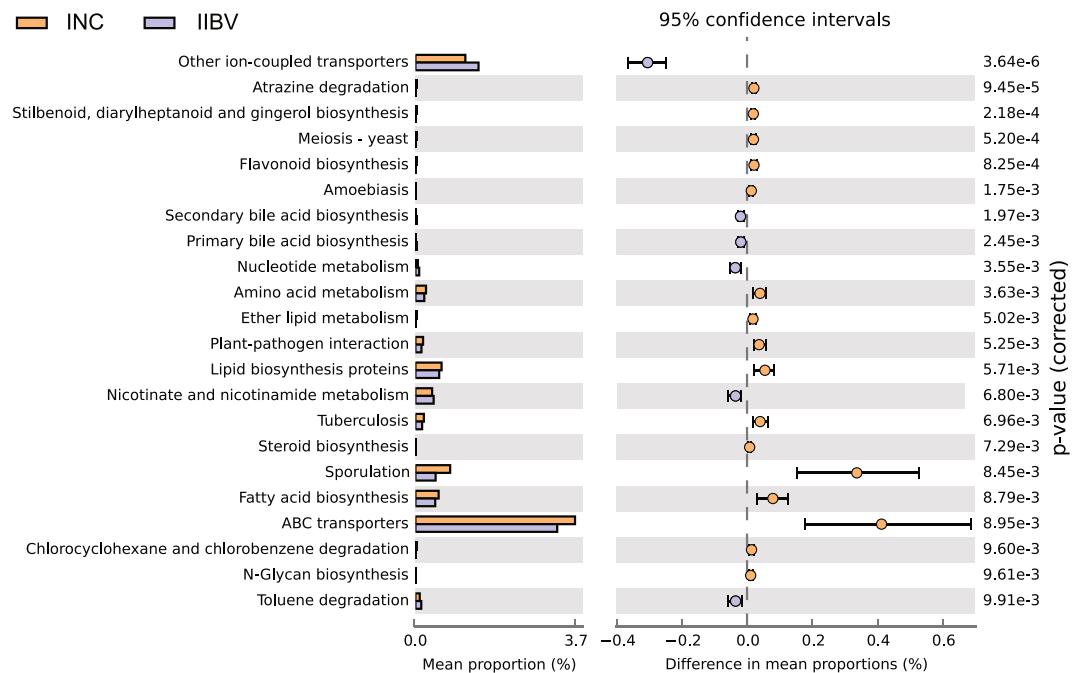


Figure 6. Predicted differential KEGG pathways in the INC and IIBV groups. The PICRUSt-predicted relative abundance of the KEGG pathways (KEGG level 3) was compared between the INC and IIBV groups. The statistical analysis was conducted using White's nonparametric t-test between the two groups, and only the significant differences in the KEGG pathways (with a P-value < 0.01) are shown.

of NIBV-infected chickens. Moreover, the LefSe results showed that *Enterobacteriaceae* belonging to the phylum *Proteobacteria* were over-represented in the IIBV group. Previous research shows that in the case of intestinal inflammation, epithelial cells reduce their capacity to undergo beta-oxidation, with the consequence of an increased availability of oxygen, which is thought to promote the bloom of *Proteobacteria* and the dysbiosis of the gut microbiota^{46,47}. Further investigations acknowledged that nitrate produced by the host during inflammatory conditions can be exploited by commensal *Enterobacteriaceae*, which thus become predominant⁴⁸. Therefore, the increased enrichment of *Proteobacteria* revealed that the intestinal inflammation in the ilea of NIBV-infected chickens represent a “microbial signature” of NIBV infection. The results also showed that NIBV infection decreased the abundance of the members of the *Cyanobacteria* in the ilea compared to that in the INC group chickens. The *Cyanobacteria* group has great biodiversity due to its secondary metabolites, which show a broad variety of biological activities, including antibacterial, antiviral, anticancer and immunomodulator or protease inhibitor activities^{28,49,50}. Our results showed a reduction in *Cyanobacteria*, which indicated that the ability of the chicken ileum to clear viruses was weakened by NIBV infection. Clearly, in the case of viral infection, changes in general metabolic function are closely related to the gain and loss of microbial populations.

Multiple studies suggest that gut microbiota influences the host metabolism^{51–53}. Cox *et al.* showed that disruption of microbiota (reduction in *Allobaculum*, *Lactobacillus*, *Rikenellaceae* and *Candidatus Arthromitus* (segmented filamentous bacteria, SFB⁵⁴)) can induce obesity⁵⁵. In the present study, we found that *Candidatus Arthromitus* was dramatically reduced in the IIBV group compared to that in the INC group. However, due to the lack of records of body weight and body fat percentage (BFP) data, it was difficult to verify the direct effect of the reduction in the abundance of *Firmicutes*, such as *Candidatus Arthromitus*, on the body in this experiment. Fortunately, in the present study, we predicted the unobserved character states in the bacterial community by using PICRUSt, which is generally applied to investigate animal intestinal function⁵⁶. With respect to the PICRUSt results, the “primary bile acid biosynthesis” and “secondary bile acid biosynthesis” pathways were significantly enriched in the ilea of the IIBV group chickens. Bile acids are cholesterol-derived compounds synthesized in the liver, and gut microbiota can transfer primary bile acids in the small intestine via deconjugation, dehydroxylation, or dehydrogenation to form so-called secondary bile acids, which promote the intestinal absorption of lipids and affect energy metabolism mainly via the farnesoid X receptor (FXR) and G protein-coupled receptor (TGR5)^{57–59}. A great number of observational studies have indicated that meta-inflammatory disorders, such as obesity and type 2 diabetes (T2D), are always associated with an increase in total bile acid (BA) concentrations^{60,61}. In addition, Annika *et al.* showed that the levels of iso-DCA, which is a common BA produced by bacteria, were significantly increased in humanized mice with low *Clostridia* abundance. As highlighted above, we know that the enrichment of bile acid biosynthesis is closely related to the loss of *Clostridia*, which may act as an important part of host metabolism in response to NIBV infections.

In conclusion, existing literature highlights the vital role of gut microbiota in the defence against viral infection. Our results suggested that relative abundance data from the ileal microbiota may differentiate the INC group chickens from the IIBV group chickens infected with NIBV. Microbiome profiles could be a biological indicator

of IBV infection; therefore, further investigation into the mechanism of this shift will help us understand IBV infection and provide a new approach to diagnose, prevent and treat infections.

Methods

Viral strains. The IBV strain was isolated in Nanchang, China in 2011 and stored by the College of Animal Science and Technology, Jiangxi Agricultural University and is designated SX9 throughout this study. At the affected farm, the diseased chickens had the same clinical symptoms: the kidney parenchyma of the dead birds was pale, swollen and mottled. These results show that the IBV strain SX9 has strong nephropathogenic characteristics. The IBV strain SX9 used in this study was propagated in 10-day-old specific-pathogen-free (SPF) embryonated eggs (Jinan saiss poultry Co., Ltd., Shandong, China) by the allantoic route. The IBV viral titer (median embryo lethal dose, ELD₅₀) was evaluated in the 10-day-old SPF eggs and calculated by the Reed-Muench method.

Experimental design. A total of 240 healthy Hy-Line variety brown chickens were randomly divided into two experimental groups: a normal group (INC) (30 chickens per subgroup) and a diseased group (IIBV) (30 chickens per subgroup). As shown in Fig. 1A, 0.2 ml of 10⁵ ELD₅₀ of SX9 was intranasally inoculated into each chicken in the IIBV group at 28 days of age, while 0.2 ml of sterile physiological saline was administered to each chicken in the INC group. Two chickens were randomly chosen per subgroup at 10 dpi and were euthanized by carbon inhalation. The livers, spleens, kidneys, ilea and jejunum were quickly separated from the bodies in a sterile environment. The ilea were isolated for morphological assessment, and ileal content samples were gathered for bacterial V3-V4 16S rRNA gene sequencing. The rest of the animals were euthanized according to the animal care guidelines of Jiangxi Agricultural University.

Viral load quantification by RT-qPCR. Total RNA was extracted from the livers, spleens, kidneys, ilea and jejunum with RNAiso Plus (Takara, Japan) following the manufacturer's protocol. The RNA was quantified using a NanoDrop 1000 Spectrophotometer (Thermo Fisher Scientific, USA). The cDNA was prepared from 2 µg of RNA. The QPCR was performed with primers (forward: 5'-CCATGGCAAGCGGTAAAGCAR-3'; reverse: 5'-CCACTCAAAGTTCATTCTCTCC-3') and a QuantStudio 7 Flex Real-Time PCR system (ABI Thermo Fisher Scientific, USA). In brief, the amplification was performed using 10 µl volume reactions in a 96-well plate format with the following conditions: 94 °C for 30 s, then 36 cycles of 94 °C for 5 s, 60 °C for 30 s and 72 °C for 30 s. The IBV RNA copy levels were quantified by comparison with a standard curve generated using dilutions (6.67 × 10³–6.67 × 10¹⁰ copies) of the IBV N gene containing plasmid. The IBV RNA levels are expressed as IBV genome copies per 0.2 µg of RNA using the standard curve.

Histopathology. Sections of the ileal tissues were stained with haematoxylin and eosin (H&E) for assessment of the general ileal morphometry. For each slice, fields were randomly selected, from which all villi were quantified by Image-Pro Plus 6.0.

16S rRNA gene sequencing. 16S rRNA gene sequencing was performed as described previously⁶². In short, the total genomic DNA in the ileal contents was first extracted, and then, using the genomic DNA as a template, the 16S rRNA gene of the V3-V4 region was amplified using specific primers (forward 341 F: CCTAYGGGRBGCASCAG and reverse 806 R: GGACTACNNGGTATCTAAT) tagged with the unique barcode. Then the desired size (approximately 400–450 bp) of the PCR products was selected to prepare the sequencing libraries, and the index codes were added. Finally, the samples were sequenced on an Illumina HiSeq. 2500 platform.

Statistical analysis of the data. Samples were created from the paired-end reads by cutting off their unique barcode and primer sequence. The paired-end reads were merged using Fast Length Adjustment of SHort reads (FLASH) software (version 1.2.7, <http://ccb.jhu.edu/software/FLASH/>)⁶³, and raw FASTQ data has been submitted in the SRA database of the NCBI with accession number PRJNA 533742. To obtain high-quality clean tags, quality filtering of the raw tags was performed using the Quantitative Insights Into Microbial Ecology software (QIIME, version 1.9.1, http://qiime.org/scripts/split_libraries_fastq.html)⁶⁴ quality-controlled process. The chimaeric sequences were removed by using the UCHIME Algorithm (http://www.drive5.com/usearch/manual/uchime_algo.html), and then the effective tags were obtained⁶⁵. The sequences were clustered into OTUs at 97% similarity by UPARSE software (version 7.0.1001, <http://drive5.com/uparse/>)²⁵. In addition, the GreenGene database and MUSCLE software (version 3.8.31, <http://www.drive5.com/muscle/>) were used to annotate the taxonomic information and conduct the multiple sequence alignment, respectively⁶⁶.

The alpha diversity index was calculated: Chao1 and ACE were used to calculate the bacterial community richness and the Shannon and Simpson indices were calculated to reflect the community diversity⁶⁷. The beta diversity index was calculated using UniFrac and Bray-Curtis distances in QIIME to compare and analyse the composition of the bacterial communities in different samples. PCoA was analysed by the “WGCNA”, “stats” and “ggplot2” packages in R. NMDS and ANOSIM were conducted using the “vegan” package, and a simpler analysis was performed by the “simpler” package. To find the differences in the biomarkers between the uninfected chickens and chickens infected with the NIBV, we performed a LEfSe analysis (<http://huttenhower.sph.harvard.edu/lefse/>)³⁰ with the following prerequisites: the p value was 0.05, and the threshold on the logarithmic linear discriminant analysis (LDA) score was 4.0^{30,68}. In addition, a Phylogenetic Investigation of Communities by Reconstruction of Unobserved States (PICRUSt, version 1.0.0, <http://picrust.github.com/>)³¹ was performed to predict the ileal microbial community function of the two groups of chickens. Finally, a statistical analysis of the taxonomic and functional profiles (STAMP, version 2.1.3, <http://kiwi.cs.dal.ca/Software/STAMP/>)⁶⁹ was used for further exploration of the results that were clustered in level 3 of the KEGG analysis module in the PICRUSt analysis.

Statistical analysis. GraphPad Prism (La Jolla, CA, USA) was used for statistical analysis and visualization. A P-value of <0.05 was considered statistically significant.

Ethical approval. The Institutional Animal Care and Use Committee of Jiangxi Agricultural University approved these animal experiments (approval ID: JXAULL-2017003), and all the animal experiments adhered rigorously to the animal care guidelines of Jiangxi Agricultural University.

Data availability

The 16S rRNA sequencing data for this study were submitted to the NCBI Sequence Read Archive (SRA) under the BioProject PRJNA 533742.

Received: 16 July 2019; Accepted: 13 February 2020;

Published online: 26 February 2020

References

1. Thaiss, C. A., Zmora, N., Levy, M. & Elinav, E. The microbiome and innate immunity. *Nature* **535**, 65–74, <https://doi.org/10.1038/nature18847> (2016).
2. Clemente, J. C., Ursell, L. K., Parfrey, L. W. & Knight, R. The impact of the gut microbiota on human health: an integrative view. *Cell* **148**, 1258–1270, <https://doi.org/10.1016/j.cell.2012.01.035> (2012).
3. Awad, W. A. *et al.* Age-Related Differences in the Luminal and Mucosa-Associated Gut Microbiome of Broiler Chickens and Shifts Associated with *Campylobacter jejuni* Infection. *Frontiers in cellular and infection microbiology* **6**, 154, <https://doi.org/10.3389/fcimb.2016.00154> (2016).
4. Huang, X., Fan, X., Ying, J. & Chen, S. Emerging trends and research foci in gastrointestinal microbiome. *Journal of translational medicine* **17**, 67, <https://doi.org/10.1186/s12967-019-1810-x> (2019).
5. Clavel, T. & Haller, D. Bacteria- and host-derived mechanisms to control intestinal epithelial cell homeostasis: implications for chronic inflammation. *Inflammatory bowel diseases* **13**, 1153–1164, <https://doi.org/10.1002/ibd.20174> (2007).
6. Bajaj, J. S. *et al.* Altered profile of human gut microbiome is associated with cirrhosis and its complications. *Journal of hepatology* **60**, 940–947, <https://doi.org/10.1016/j.jhep.2013.12.019> (2014).
7. Qin, N. *et al.* Alterations of the human gut microbiome in liver cirrhosis. *Nature* **513**, 59–64, <https://doi.org/10.1038/nature13568> (2014).
8. Wang, B. *et al.* Altered Fecal Microbiota Correlates with Liver Biochemistry in Nonobese Patients with Non-alcoholic Fatty Liver Disease. *Scientific reports* **6**, 32002, <https://doi.org/10.1038/srep32002> (2016).
9. Hooper, L. V. *et al.* Molecular analysis of commensal host-microbial relationships in the intestine. *Science* **291**, 881–884, <https://doi.org/10.1126/science.291.5505.881> (2001).
10. O'Hara, A. M. & Shanahan, F. The gut flora as a forgotten organ. *EMBO reports* **7**, 688–693, <https://doi.org/10.1038/sj.embor.7400731> (2006).
11. Thomas, A. M. *et al.* Tissue-Associated Bacterial Alterations in Rectal Carcinoma Patients Revealed by 16S rRNA Community Profiling. *Frontiers in cellular and infection microbiology* **6**, 179, <https://doi.org/10.3389/fcimb.2016.00179> (2016).
12. Shang, Y., Kumar, S., Thippareddi, H. & Kim, W. K. Effect of Dietary Fructooligosaccharide (FOS) Supplementation on Ileal Microbiota in Broiler Chickens. *Poultry science* **97**, 3622–3634, <https://doi.org/10.3382/ps/pey131> (2018).
13. Gong, J. *et al.* 16S rRNA gene-based analysis of mucosa-associated bacterial community and phylogeny in the chicken gastrointestinal tracts: from crops to ceca. *FEMS microbiology ecology* **59**, 147–157, <https://doi.org/10.1111/j.1574-6941.2006.00193.x> (2007).
14. Zilberman-Schapira, G. *et al.* The gut microbiome in human immunodeficiency virus infection. *BMC medicine* **14**, 83, <https://doi.org/10.1186/s12916-016-0625-3> (2016).
15. Sui, Y. *et al.* Influence of gut microbiome on mucosal immune activation and SHIV viral transmission in naive macaques. *Mucosal immunology* **11**, 1219–1229, <https://doi.org/10.1038/s41385-018-0029-0> (2018).
16. Carstens, E. B. Report from the 40th meeting of the Executive Committee of the International Committee of Taxonomy of Viruses. *Archives of Virology* **154**, 1571–1574, <https://doi.org/10.1007/s00705-009-0458-x> (2009).
17. Feng, J. *et al.* Virulent avian infectious bronchitis virus, People's Republic of China. *Emerging infectious diseases* **18**, 1994–2001, <https://doi.org/10.3201/eid1812.120552> (2012).
18. Han, Z. *et al.* A 15-year analysis of molecular epidemiology of avian infectious bronchitis coronavirus in China. *Infection, genetics and evolution: journal of molecular epidemiology and evolutionary genetics in infectious diseases* **11**, 190–200, <https://doi.org/10.1016/j.meegid.2010.09.002> (2011).
19. Raj, G. D. & Jones, R. C. Immunopathogenesis of infection in SPF chicks and commercial broiler chickens of a variant infectious bronchitis virus of economic importance. *Avian pathology: journal of the W.V.P.A* **25**, 481–501, <https://doi.org/10.1080/03079459608419157> (1996).
20. Stanley, D., Hughes, R. J. & Moore, R. J. Microbiota of the chicken gastrointestinal tract: influence on health, productivity and disease. *Applied microbiology and biotechnology* **98**, 4301–4310, <https://doi.org/10.1007/s00253-014-5646-2> (2014).
21. Mohd Shaufi, M. A., Sieo, C. C., Chong, C. W., Gan, H. M. & Ho, Y. W. Deciphering chicken gut microbial dynamics based on high-throughput 16S rRNA metagenomics analyses. *Gut pathogens* **7**, 4, <https://doi.org/10.1186/s13099-015-0051-7> (2015).
22. Biggs, P. & Parsons, C. M. The effects of several organic acids on growth performance, nutrient digestibilities, and cecal microbial populations in young chicks. *Poultry science* **87**, 2581–2589, <https://doi.org/10.3382/ps.2008-00080> (2008).
23. Sogin, M. L. *et al.* Microbial diversity in the deep sea and the underexplored “rare biosphere”. *Proceedings of the National Academy of Sciences of the United States of America* **103**, 12115–12120, <https://doi.org/10.1073/pnas.0605127103> (2006).
24. Avellaneda, G. E., Villegas, P., Jackwood, M. W. & King, D. J. *In vivo* evaluation of the pathogenicity of field isolates of infectious bronchitis virus. *Avian diseases* **38**, 589–597 (1994).
25. Edgar, R. C. UPARSE: highly accurate OTU sequences from microbial amplicon reads. *Nature methods* **10**, 996–998, <https://doi.org/10.1038/nmeth.2604> (2013).
26. Koren, O. *et al.* A guide to enterotypes across the human body: meta-analysis of microbial community structures in human microbiome datasets. *Plos computational biology* **9**, e1002863, <https://doi.org/10.1371/journal.pcbi.1002863> (2013).
27. Noval Rivas, M. *et al.* A microbiota signature associated with experimental food allergy promotes allergic sensitization and anaphylaxis. *The Journal of allergy and clinical immunology* **131**, 201–212, <https://doi.org/10.1016/j.jaci.2012.10.026> (2013).
28. Ma, X. *et al.* 16S rRNA genes Illumina sequencing revealed differential cecal microbiome in specific pathogen free chickens infected with different subgroup of avian leukosis viruses. *Veterinary microbiology* **207**, 195–204, <https://doi.org/10.1016/j.vetmic.2017.05.016> (2017).
29. Excoffier, L., Smouse, P. E. & Quattro, J. M. Analysis of molecular variance inferred from metric distances among DNA haplotypes: application to human mitochondrial DNA restriction data. *Genetics* **131**, 479–491 (1992).
30. Segata, N. *et al.* Metagenomic biomarker discovery and explanation. *Genome biology* **12**, R60, <https://doi.org/10.1186/gb-2011-12-6-r60> (2011).

31. Langille, M. G. *et al.* Predictive functional profiling of microbial communities using 16S rRNA marker gene sequences. *Nature biotechnology* **31**, 814–821, <https://doi.org/10.1038/nbt.2676> (2013).
32. Flint, H. J., Scott, K. P., Louis, P. & Duncan, S. H. The role of the gut microbiota in nutrition and health. *Nature reviews. Gastroenterology & hepatology* **9**, 577–589, <https://doi.org/10.1038/nrgastro.2012.156> (2012).
33. Zhu, L., Liao, R., Wu, N., Zhu, G. & Yang, C. Heat stress mediates changes in fecal microbiome and functional pathways of laying hens. *Applied microbiology and biotechnology* **103**, 461–472, <https://doi.org/10.1007/s00253-018-9465-8> (2019).
34. Huang, T. *et al.* Temporal Effects of High Fishmeal Diet on Gut Microbiota and Immune Response in Clostridium perfringens-Challenged Chickens. *Frontiers in microbiology* **9**, 2754, <https://doi.org/10.3389/fmicb.2018.02754> (2018).
35. Pandit, R. J. *et al.* Microbial diversity and community composition of caecal microbiota in commercial and indigenous Indian chickens determined using 16s rDNA amplicon sequencing. *Microbiome* **6**, 115, <https://doi.org/10.1186/s40168-018-0501-9> (2018).
36. Wang, W. *et al.* Effects of Kluyveromyces marxianus supplementation on immune responses, intestinal structure and microbiota in broiler chickens. *Plos one* **12**, e0180884, <https://doi.org/10.1371/journal.pone.0180884> (2017).
37. Gangadoo, S. *et al.* Selenium nanoparticles in poultry feed modify gut microbiota and increase abundance of Faecalibacterium prausnitzii. *Applied microbiology and biotechnology* **102**, 1455–1466, <https://doi.org/10.1007/s00253-017-8688-4> (2018).
38. Johansson, M. E., Sjovall, H. & Hansson, G. C. The gastrointestinal mucus system in health and disease. *Nature reviews. Gastroenterology & hepatology* **10**, 352–361, <https://doi.org/10.1038/nrgastro.2013.35> (2013).
39. Chairatana, P. & Nolan, E. M. Defensins, lectins, mucins, and secretory immunoglobulin A: microbe-binding biomolecules that contribute to mucosal immunity in the human gut. *Critical reviews in biochemistry and molecular biology* **52**, 45–56, <https://doi.org/10.1080/10409238.2016.1243654> (2017).
40. Thim, L. & May, F. E. Structure of mammalian trefoil factors and functional insights. *Cellular and molecular life sciences: CMLS* **62**, 2956–2973, <https://doi.org/10.1007/s00018-005-5484-6> (2005).
41. Yildiz, S., Mazel-Sanchez, B., Kandasamy, M., Manicassamy, B. & Schmolke, M. Influenza A virus infection impacts systemic microbiota dynamics and causes quantitative enteric dysbiosis. *Microbiome* **6**, 9, <https://doi.org/10.1186/s40168-017-0386-z> (2018).
42. Kang, D. W. *et al.* Reduced incidence of Prevotella and other fermenters in intestinal microflora of autistic children. *Plos one* **8**, e68322, <https://doi.org/10.1371/journal.pone.0068322> (2013).
43. El-Far, M. & Tremblay, C. L. Gut microbial diversity in HIV infection post combined antiretroviral therapy: a key target for prevention of cardiovascular disease. *Current opinion in HIV and AIDS* **13**, 38–44, <https://doi.org/10.1097/COH.0000000000000426> (2018).
44. Qin, N. *et al.* Influence of H7N9 virus infection and associated treatment on human gut microbiota. *Scientific reports* **5**, 14771, <https://doi.org/10.1038/srep14771> (2015).
45. Huang, A. *et al.* Dynamic Change of Gut Microbiota During Porcine Epidemic Diarrhea Virus Infection in Suckling Piglets. *Frontiers in microbiology* **10**, 322, <https://doi.org/10.3389/fmicb.2019.00322> (2019).
46. Hughes, E. R. *et al.* Microbial Respiration and Formate Oxidation as Metabolic Signatures of Inflammation-Associated Dysbiosis. *Cell host & microbe* **21**, 208–219, <https://doi.org/10.1016/j.chom.2017.01.005> (2017).
47. Litvak, Y., Byndloss, M. X., Tsolis, R. M. & Bauml, A. J. Dysbiotic Proteobacteria expansion: a microbial signature of epithelial dysfunction. *Current opinion in microbiology* **39**, 1–6, <https://doi.org/10.1016/j.mib.2017.07.003> (2017).
48. Winter, S. E. *et al.* Host-derived nitrate boosts growth of *E. coli* in the inflamed gut. *Science* **339**, 708–711, <https://doi.org/10.1126/science.1232467> (2013).
49. Singh, R. K., Tiwari, S. P., Rai, A. K. & Mohapatra, T. M. Cyanobacteria: an emerging source for drug discovery. *The Journal of antibiotics* **64**, 401–412, <https://doi.org/10.1038/ja.2011.21> (2011).
50. Raja, R., Hemaiswarya, S., Ganesan, V. & Carvalho, I. S. Recent developments in therapeutic applications of Cyanobacteria. *Critical reviews in microbiology* **42**, 394–405, <https://doi.org/10.3109/1040841X.2014.957640> (2016).
51. Turnbaugh, P. J. *et al.* An obesity-associated gut microbiome with increased capacity for energy harvest. *Nature* **444**, 1027–1031, <https://doi.org/10.1038/nature05414> (2006).
52. Ridaura, V. K. *et al.* Gut microbiota from twins discordant for obesity modulate metabolism in mice. *Science* **341**, 1241214, <https://doi.org/10.1126/science.1241214> (2013).
53. Sonnenburg, J. L. & Backhed, F. Diet-microbiota interactions as moderators of human metabolism. *Nature* **535**, 56–64, <https://doi.org/10.1038/nature18846> (2016).
54. Thompson, C. L., Vier, R., Mikaelyan, A., Wienemann, T. & Brune, A. ‘Candidatus Arthromitus’ revised: segmented filamentous bacteria in arthropod guts are members of Lachnospiraceae. *Environmental microbiology* **14**, 1454–1465, <https://doi.org/10.1111/j.1462-2920.2012.02731.x> (2012).
55. Cox, L. M. *et al.* Altering the intestinal microbiota during a critical developmental window has lasting metabolic consequences. *Cell* **158**, 705–721, <https://doi.org/10.1016/j.cell.2014.05.052> (2014).
56. Fuentes, S. *et al.* Microbial shifts and signatures of long-term remission in ulcerative colitis after faecal microbiota transplantation. *The ISME journal* **11**, 1877–1889, <https://doi.org/10.1038/ismej.2017.44> (2017).
57. Just, S. *et al.* The gut microbiota drives the impact of bile acids and fat source in diet on mouse metabolism. *Microbiome* **6**, 134, <https://doi.org/10.1186/s40168-018-0510-8> (2018).
58. Haeusler, R. A. *et al.* Increased Bile Acid Synthesis and Impaired Bile Acid Transport in Human Obesity. *The Journal of clinical endocrinology and metabolism* **101**, 1935–1944, <https://doi.org/10.1210/jc.2015-2583> (2016).
59. Ridlon, J. M., Kang, D. J. & Hylemon, P. B. Bile salt biotransformations by human intestinal bacteria. *Journal of lipid research* **47**, 241–259, <https://doi.org/10.1194/jlr.R500013-JLR200> (2006).
60. Guo, C. *et al.* Bile Acids Control Inflammation and Metabolic Disorder through Inhibition of NLRP3 Inflammasome. *Immunity* **45**, 802–816, <https://doi.org/10.1016/j.immuni.2016.09.008> (2016).
61. Sonne, D. P. *et al.* Postprandial Plasma Concentrations of Individual Bile Acids and FGF-19 in Patients With Type 2 Diabetes. *The Journal of clinical endocrinology and metabolism* **101**, 3002–3009, <https://doi.org/10.1210/jc.2016-1607> (2016).
62. Xu, P. *et al.* A Multi-Omics Study of Chicken Infected by Nephropathogenic Infectious Bronchitis Virus. *Viruses* **11**, 1070, <https://doi.org/10.3390/v11111070> (2019).
63. Magoc, T. & Salzberg, S. L. FLASH: fast length adjustment of short reads to improve genome assemblies. *Bioinformatics* **27**, 2957–2963, <https://doi.org/10.1093/bioinformatics/btr507> (2011).
64. Caporaso, J. G. *et al.* QIIME allows analysis of high-throughput community sequencing data. *Nature methods* **7**, 335–336, <https://doi.org/10.1038/nmeth.f.303> (2010).
65. Edgar, R. C., Haas, B. J., Clemente, J. C., Quince, C. & Knight, R. UCHIME improves sensitivity and speed of chimera detection. *Bioinformatics* **27**, 2194–2200, <https://doi.org/10.1093/bioinformatics/btr381> (2011).
66. Edgar, R. C. MUSCLE: multiple sequence alignment with high accuracy and high throughput. *Nucleic acids research* **32**, 1792–1797, <https://doi.org/10.1093/nar/gkh340> (2004).
67. Schloss, P. D. & Handelsman, J. Introducing DOTUR, a computer program for defining operational taxonomic units and estimating species richness. *Applied and environmental microbiology* **71**, 1501–1506, <https://doi.org/10.1128/AEM.71.3.1501-1506.2005> (2005).
68. Tang, R. *et al.* 16S rRNA gene sequencing reveals altered composition of gut microbiota in individuals with kidney stones. *Urolithiasis* **46**, 503–514, <https://doi.org/10.1007/s00240-018-1037-y> (2018).
69. Parks, D. H., Tyson, G. W., Hugenholtz, P. & Beiko, R. G. STAMP: statistical analysis of taxonomic and functional profiles. *Bioinformatics* **30**, 3123–3124, <https://doi.org/10.1093/bioinformatics/btu494> (2014).

Acknowledgements

The authors would like to gratefully acknowledge all the team members of the clinical veterinary medicine laboratory (Jiangxi Agricultural University) for helpful discussions and technical support. We also thank Vincent Latigo for the favour of addressing the grammar issues in the manuscript. This study was supported by the National Natural Science Foundation of China (Grant No. 31860723) and the Key Programs of the Natural Science Foundation of Jiangxi Province of China (Grant No. 2017ACB20012).

Author contributions

X.G. conceived and supervised the study. X.G. acquired funding; P.X., P.L., C.M.Z., G.L. and Y.S. performed the data analysis. P.X., Y.Y., C.Y.Z., J.L. and H.C. performed the animal study and/or contributed materials. P.X. and Y.S. prepared the manuscript draft. P.L., X.G. and G.H. revised the manuscript and provided extensive discussions. All authors participated in discussion and editing of the manuscript.

Competing interests

The authors declare no competing interests.

Additional information

Correspondence and requests for materials should be addressed to X.G.

Reprints and permissions information is available at www.nature.com/reprints.

Publisher's note Springer Nature remains neutral with regard to jurisdictional claims in published maps and institutional affiliations.



Open Access This article is licensed under a Creative Commons Attribution 4.0 International License, which permits use, sharing, adaptation, distribution and reproduction in any medium or format, as long as you give appropriate credit to the original author(s) and the source, provide a link to the Creative Commons license, and indicate if changes were made. The images or other third party material in this article are included in the article's Creative Commons license, unless indicated otherwise in a credit line to the material. If material is not included in the article's Creative Commons license and your intended use is not permitted by statutory regulation or exceeds the permitted use, you will need to obtain permission directly from the copyright holder. To view a copy of this license, visit <http://creativecommons.org/licenses/by/4.0/>.

© The Author(s) 2020